Novel inductively-heated catalytic system for fast VOCs abatement, application to IPA in air

J. Leclercq [a], F. Giraud [a], D. Bianchi [a], K. Fiaty [b], F. Gaillard [a],*

[a] *Institut de Recherches sur la Catalyse et l'Environnement de Lyon (IRCELYON), UMR 5256 CNRS – Université Claude Bernard Lyon 1, 2 avenue Albert Einstein, 69626, Villeurbanne cedex, France*
[b] *Laboratoire d'Automatique et de Génie des Procédés (LAGEP), UMR 5007CNRS – Université Claude Bernard Lyon 1, ESCPE-Lyon, 43 bd du 11 N ovembre 1918, 69622, Villeurbanne cedex, France*

ABSTRACT

Pt-Al_2O_3, Al_2O_3 and SnO_2 were deposited as thin films on a stainless steel support that was inserted into an annular reactor and heated using an electromagnetic induction device. Possibility of an accurate temperature control was demonstrated and heating rates up to $800\,°C\,min^{-1}$ were obtained. Total abatement of 1000 ppm isopropyl alcohol (IPA) was achieved at low temperature (T50 about $80\,°C$) on 1 wt% Pt/Al_2O_3. Nevertheless, the strong IPA adsorption on the alumina support and the formation of large amounts of acetone dictated to select the other catalyst, SnO_2. IPA 90% conversion into CO_2 and H_2O was then obtained at $250\,°C$ with a total flow of $100\,NmL\,min^{-1}$ containing 1000 ppm IPA. Considering the volume of the very thin reactive sheath (hydraulic diameter about 3.6 mm), *ghsv* was as high as $2.6 \times 10^3\,h^{-1}$. Total abatement to CO_2 and H_2O of high amounts of IPA (about 1 vol%) in air was achieved in less than 30 s and near-room temperature was recovered quickly when the contaminant level at the reactor inlet felled again below a given threshold

© 2013 Elsevier B.V. All rights reserved.

1. Introduction

From the beginning of the 21st century, due to increasing social and political concern in environment, the removal of volatile organic compounds (VOCs) emitted from industrial and domestic processes has drawn a lot of attention. A cheap and efficient way of VOCs removing is their complete catalytic oxidation to harmless products such as H_2O and CO_2 [1]. Catalytic oxidation is an efficient process but it generally requires to heat large amounts of air at quite high temperatures (i.e. 200–400 °C). Treating large volumes by catalytic oxidation can be relatively expensive. Mere thermal incineration is also energy-consuming and is likely to generate undesirable byproducts [2]. Photocatalysis [3], possibly combined to biological treatment [4], shows good performance for indoor air treatment at room temperature but is devoted to low contamination levels (ppb–ppm levels) and suffers from low reaction rate [5]. Filtration/adsorption [6] can be used but needs to process the used sorbent. Finally plasma techniques [7] and especially nonthermal plasma [8] may be a promising choice and have been considered as effective and energy-saving methods for VOCs abatement.

Anyway, some circumstances necessitate a fast and total oxidation of VOCs. It is for example the case of accidental contamination of working places, or the treatment of a sorbent by temperature swing regeneration (TSR) [9]. This last process is generally considered as slow and some solutions like microwaves heating have been proposed to intensify the desorption processes [10]. Therefore new heating systems can be a solution for catalytic devices in intermittent use or systems needing fast operation to remove accidental pollution. For this purpose, inductive heating can be a good candidate. It has shown its ability to heat very quickly and homogeneously metallic pieces such as stainless steel plates or tubes [11] which are very well-suited as catalyst structured support.

The purpose of this paper is to show the first application of an inductive system for very fast heating of Al_2O_3/stainless steel, Pt-Al_2O_3/stainless steel, and SnO_2/stainless steel assemblies used for the abatement of isopropyl alcohol (IPA) in air. IPA is a very interesting compound for such a study. First of all, it is a very common VOC which is much used in offset lithographic printing [12], as a cleaner and solvent for coatings [13], for industrial processes in pharmaceutical applications or for processing oilseeds [14]. A significant fraction is also consumed for household use and in personal care products [15]. Selectivity in the decomposition reaction of IPA has long been regarded as a typical reaction for investigating the acid–base properties of the catalytic sites of metal oxides [16]. The dehydrogenation (to acetone) of IPA was assumed to occur on the surface basic sites and the dehydration (to propene) on the acid sites on the surface of the catalyst. Anyway, selectivity to acetone was shown to depend on oxygen and water in the feed stream [17]

* Corresponding author. Tel.: +33 472 448 066; fax: +33 472 445 399.
E-mail address: francois.gaillard@ircelyon.univ-lyon1.fr (F. Gaillard).
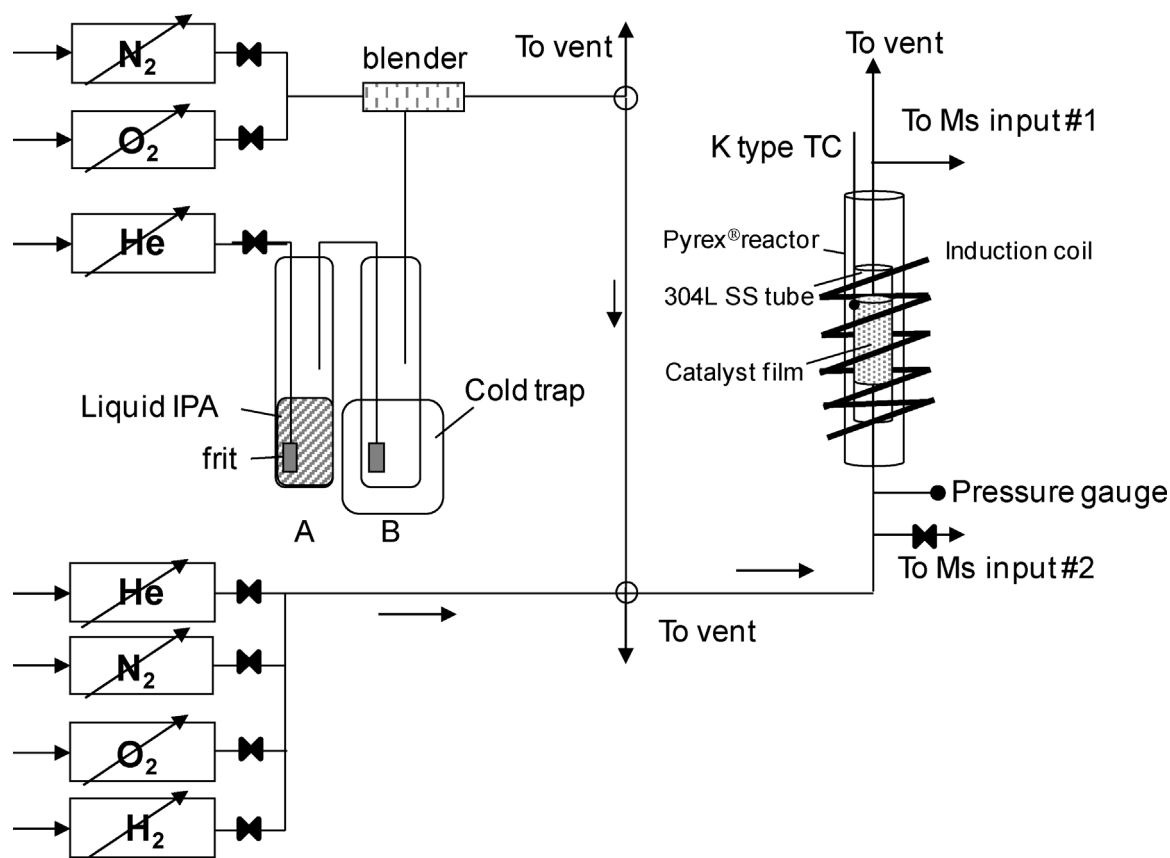
Fig. 1. Schematic drawing of the experimental setup.

and the use of IPA as an acid–base probe needs some adjustments [18]. Nevertheless, IPA is a common organic solvent that is utilized as an industrial raw material and a good candidate to evaluate de feasibility of VOC abatement in an inductively-heated catalytic reactor

2. Experimental

2.1. Materials

The selected VOC was isopropyl alcohol (IPA, HPLC Grade, from Sigma–Aldrich). Carrier gas was 80%vol% N_2 (or 80 vol% N_2–10 vol% He when IPA was added to the flow) and 20 vol% O_2 to mimic air and then being close to the real application. The catalyst support was an AISI 304 L austenitic stainless steel (SS) tube 6.35 mm in o.d. (Swagelok) and 50 mm in length. Numerous methods to deposit catalysts on structured surfaces were reviewed recently by Meille [19]. We selected electrophoretic deposition (EPD) which consists in a colloidal process wherein a direct current is imposed between the sample to coat and a stainless steel or aluminium anode. This method was successfully used, for example, by Wunsh et al. [20] to coat microchannels with Al_2O_3 nanoparticles.

The external part of the stainless steel tube was coated with the investigated materials by EPD from suspensions of the corresponding materials. For each material to be deposited, optimized operating modes and deposit mechanisms were reported in the literature. We selected an acetone/ethanol with I_2 addition bath for SnO_2 [21] and a $C_2H_5OH + HCl$ (pH 3) bath for Al_2O_3 [22]. Prior to deposition, SS was pickled in 5 vol%HF–15 vol%HNO$_3$ mixture at room temperature during 10 minutes in order to remove residual oxides and contaminants [23]. Materials to be deposited were Al_2O_3 (γ-alumina, Degussa, SSA 92 m^2 g^{-1}) as a common catalyst support,

1 w%Pt–Al_2O_3 (obtained by incipient wetness impregnation ex $H_2PtCl_6\cdot6H_2O$ from Alfa Aesar in aqueous solution, solid calcined at 450 °C in air) as a very common oxidation catalyst and SnO_2 (99.9%, 325 mesh, from Sigma–Aldrich, BET surface area 6.8 m^2 g^{-1}), which is known as a fair oxidation catalyst able to reversible oxygen adsorption/desorption exchange process and very stable during high temperature incursion [24].

2.2. Experimental setup

A schematic drawing of the experimental setup is shown in Fig. 1. Synthetic air flow was controlled by two mass flowmeters (each one selectable in the range: 10–100 NmL min^{-1}) and mixed to an He flow (controlled by a mass flowmeter in the range 1–10 NmL min^{-1}) passed through a saturator/condenser enabling to set the IPA concentration in the final mixture by acting on He flow and/or condenser temperature (generally in melting ice corresponding to an IPA vapour pressure of 8.9 Torr [25]). Operating conditions for the present work were in the range 50–125 NmL min^{-1} total flow and 1000 ppm or 1 vol%. IPA. The mixture can be directed toward a reactor of annular type [26]. Many papers were devoted to the use and the modeling of annular reactors, which are well suited to obtain kinetic data from systems operated under high *ghsv* conditions [27–29]. The reactor used for this study is depicted in Fig. 2. The outer part made of Pyrex® glass (10 mm inner dia.) and the inner part of the 304L SS tube (6.35 mm in dia.) obstructed at both the extremities in order to force the reactant flow into the gap between glass and catalyst film. The SS tube is kept in a perfectly aligned position by a ceramic tube (mullite, from SCERAM, France) passing though the reactor head. The gap between glass and catalyst film is 1.8 mm and consequently the volume of the reactive sheath is about 2.3 cm^3. Corresponding *ghsv* at a total
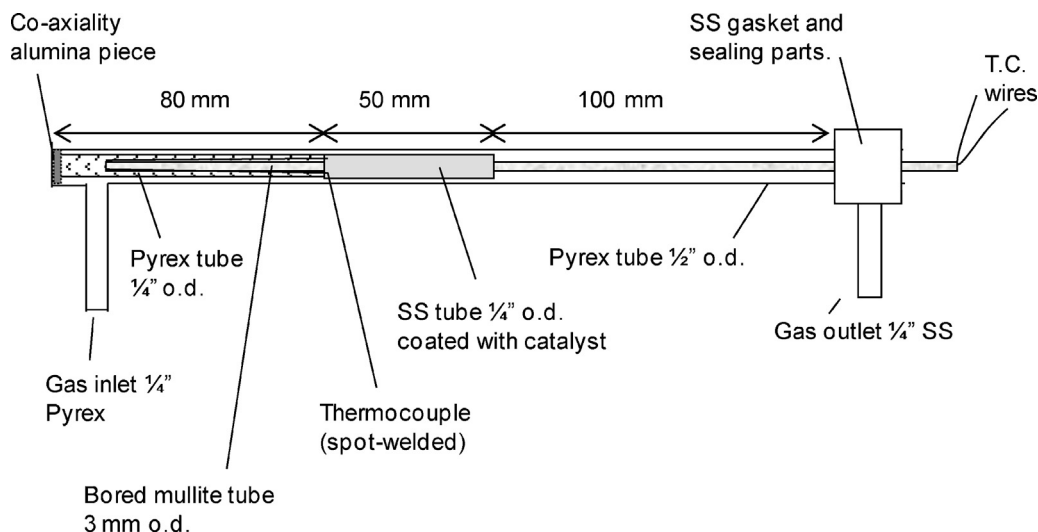
Fig. 2. Schematic drawing of the annular reactor.

flow rate of 100 NmL min^{-1} is about 2.6×10^3 h^{-1} if we refer to the volume of the reactive sheath or about 1.4×10^6 h^{-1} if we refer to a standard catalyst deposit (20 mg of Pt–Al$_2$O$_3$). Two wires, 0.125 mm in dia. and forming a capillary K-type thermocouple (from Goodfellow) were guided in bores drilled inside the ceramic tube and spot-welded at the surface of the SS tube. This allows measuring the steel temperature very accurately and with a very low inertia. Gas analysis was performed by using a MS quadrupolaire spectrometer Hiden HPR-20 QIC system, equipped with a switchable dual inlet allowing either to check gas mixture at the reactor inlet (input #2) or to analyze reaction products (input #1). The heating device for the catalytic reactor was a 400 kHz "Power Cube 32" from CEIA, interfaced to a "Power-C-V3" control system and fitted with a tailor made 5-turn induction coil outside the reactor [30]. Temperature regulation was achieved by a PID system (Eurotherm model 3504) reading sample temperature by means of the K-type thermocouple spot-welded on the stainless steel tube. Temperature of gases exiting the reactor was also recorded.

3. Results and discussion

3.1. Heating of the catalyst support

First of all, it was necessary to determine the performance and the limitation of the electromagnetic induction heating system. For this purpose, the SS catalyst support alone was inserted into the annular reactor and N$_2$ flow was set at 100 NmL min^{-1}. After determining the optimal PID parameters for this system at 250 °C, different heating rates were programmed and the resulting temperature *vs* time plots are shown in Fig. 3 for 400 (a), 200(b), 100(c), 50 (d), and 20 (e)°C min^{-1} up to a plateau at 400 °C. The mean heating rate value obtained within the range from r.t. to 400 °C is in very good agreement with the desired value: 20.01 (for 20.0), 50.04 (for 50.0), 100.2 (for 100.0), 200.6 (for 200.0) and 399.3 (for 400)°C min^{-1}, with *R* value exceeding 99.9% in all cases. The inset of Fig. 3 shows that temperature overshoot at the beginning of the plateau only occurs for the two higher heating rates and is very limited, i.e. 2 °C during 25 s at 400 °C min^{-1}. The very low thermal inertia of this system allows also controlling the cooling rate up to 100 °C min^{-1}, for temperatures higher than 100 °C or so. For lower temperatures, the natural cooling of the system remains the limiting step.

Additional experiments (not reported here) were carried out in order to be sure that temperature measured at the middle of

the SS tube (capillary thermocouple spot-welded on the external part of the tube) did not deviate from the set point during the heating ramp. Such a discrepancy can be neglected at 20, 50, and 100 °C min^{-1}, is lower than 2 °C at 200 °C min^{-1} and becomes significant at 400 °C min^{-1}, without overrunning 5 °C. In order to have valuable results, we also checked that the longitudinal temperature gradient was also kept as low as possible. Differences of temperature measured at the middle of the SS tube (outside) and at one extremity of the tube (outside) vs time for different heating rates never exceeded 10 °C and can be probably attributed to the fact that the extremities undergo a higher heat exchange combined to a lower efficiency of the electromagnetic induction at coil extremities. This fact was previously observed on a vacuum TPD system implementing inductive heating and can be cured, if necessary, by modifying the induction coil (extremity turns must be made a bit closer) [11].

3.2. IPA conversion on various catalysts deposited on SS.

In order to evaluate the performance of the system in catalytic abatement of IPA in air, we compared the SS tube covered with Al$_2$O$_3$, Pt–Al$_2$O$_3$ and SnO$_2$. Deposits amounts were 16, 16, and 31 mg, corresponding to estimated thicknesses 4, 4, and 4.5 μm, respectively. First, the reactor was fed at room temperature with

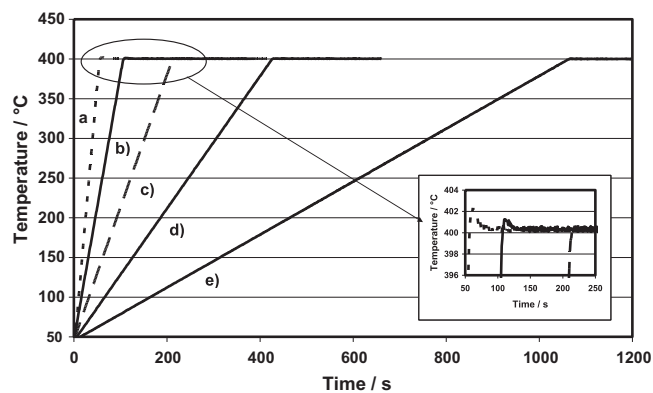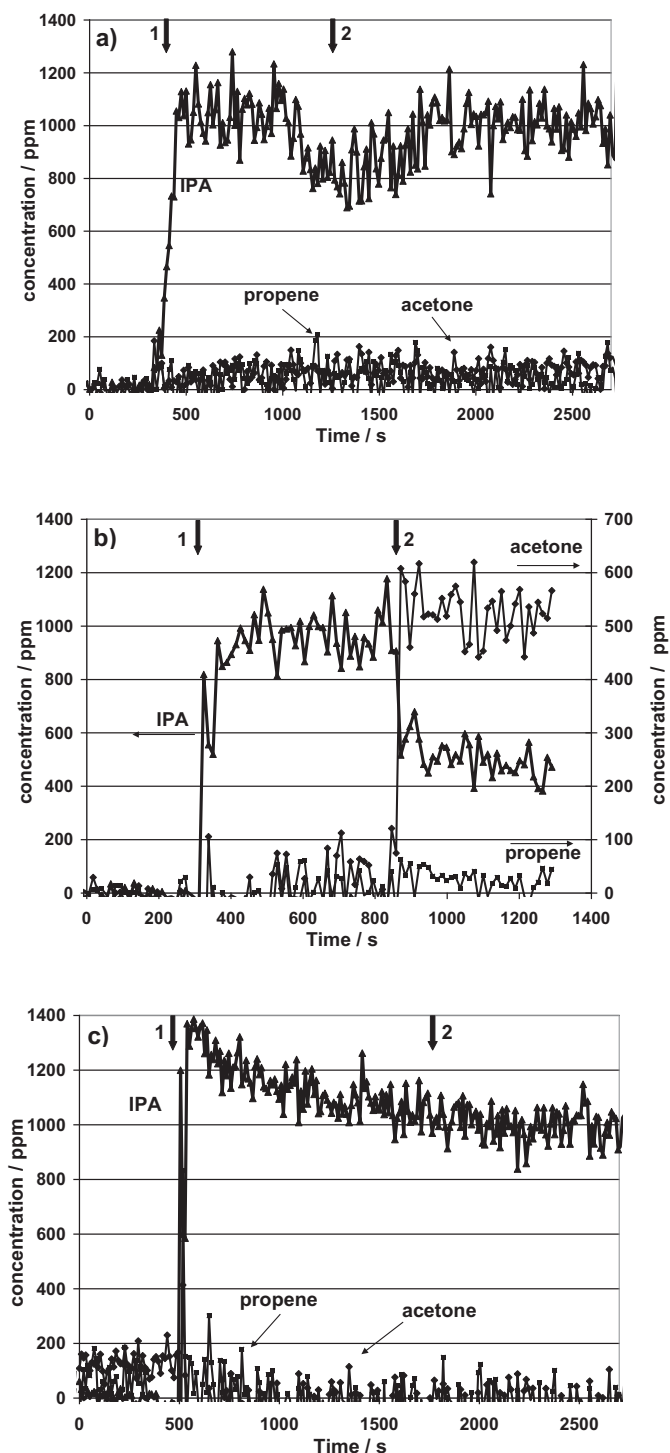**Fig. 3.** Heating of the SS catalyst support at 400 (a), 200(b), 100(c), 50 (d), and 20 (e)°C min^{-1} up to a plateau at 400 °C. The inset shows temperature overshoot at the beginning of the plateau for the three higher heating rates. N$_2$ flow rate was 100 NmL min^{-1}.

Fig. 4. Concentration variations of IPA (▲), acetone (♦) and propene (■) when feeding the reactor at room temperature with 1000 ppm IPA in air on the SS tube covered with Al_2O_3 (a), $Pt-Al_2O_3$ (b) and SnO_2 (c). Total flow rate was 100 NmL min^{-1}. Mark 1 denotes starting analysis at reactor inlet and mark 2 starting analysis at reactor outlet.

1000 ppm IPA in air (total flow rate 100 NmL min^{-1}) during 1 hour without MS analysis. Plots in Fig. 4 show concentration variations of IPA, acetone and propene *vs* time for the three catalysts: acetone and propene are well-known by-products of the interaction of IPA with catalytic solids, and their usefulness in determining acid–base properties of materials was the subject of a large amount of literature [16,31–34]. At the time marked 1 on the plot, the
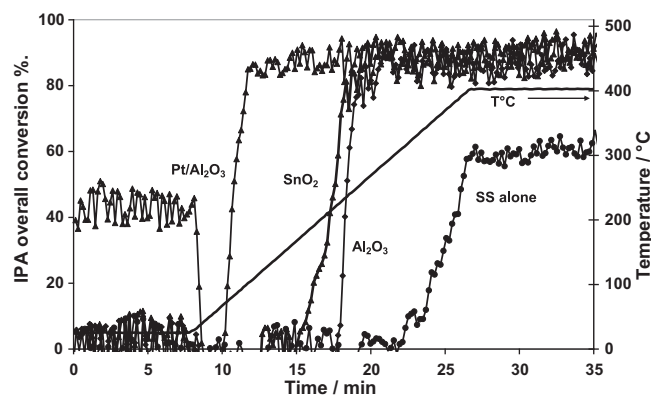
Fig. 5. Catalyst temperature and overall IPA conversion *vs* time on SS tube (●), Al_2O_3 on SS (♦), SnO_2 on SS (■), and $Pt-Al_2O_3$ on SS (▲). IPA initial concentration: 1000 ppm, heating rate: 20 °C min^{-1} and total flow rate: 100 NmL min^{-1}.

composition of the reactant flow was determined through MS input#2 following the mass peaks at $m/e = 4$, 18, 32, 41, 43, 44, and 45 amu, corresponding to helium, water, oxygen, propene, acetone, carbone dioxide and IPA, respectively.

At the time marked 2 on the plot, the gas mixture at the outlet of the reactor was analyzed through MS input#1. We can observe a marked difference between the two oxide films (SnO_2 and Al_2O_3) and $Pt-Al_2O_3$. On oxide films there is no obvious difference of composition between the inlet gas flow and the outlet gas flow. We can consider that the coverage of surfaces reach a steady state as evidenced by the IPA concentration constant around 1000 ppm. The situation is completely different with $Pt-Al_2O_3$ were IPA level is decreased to 500 ppm and acetone is continuously detected at 500 ppm level or so while no significant production of neither propene nor CO_2 was detected. This indicates a continuous IPA dehydrogenation to form acetone on $Pt-Al_2O_3$ under our experimental conditions.

After checking for signal stabilization, the temperature was increased at 20 °C min^{-1} and gas phase at the reactor outlet continuously analyzed.

Fig. 5 shows the overall IPA conversion *vs* temperature on SS tube, Al_2O_3 on SS, SnO_2 on SS, and $Pt-Al_2O_3$ on SS. The overall IPA conversion was calculated as: $(([IPA]_{t_0} - [IPA]_t)/[IPA]_{t_0}) \times 100$, irrespectively of the nature of reaction products. The choice of this calculation method explains some largely negative conversion values at the beginning of some of the light-off curves. This is due to IPA desorption from the investigated solids (especially observed with $Pt-Al_2O_3$ and Al_2O_3) leading to IPA concentration in the flow higher than the initial 1000 ppm value. This point is discussed further in the paper.

On SS alone, IPA conversion increases from 300–350 °C to reach 60% at 400 °C. Nevertheless, analysis of reaction products shows that mainly acetone is formed and no CO_2 was detected. It is interesting to note that IPA conversion on SS alone is favored after some cycles between 30 and 400 °C, resulting in an oxidized SS surface as evidence by a yellow coloration corresponding to the formation of a 20–30 nm thick chromium-enriched surface oxide film [35]. Such a chromium-rich film has been shown exhibiting acidic properties [36] which enhance their reactivity towards some organic molecules [37]. As expected, $Pt-Al_2O_3$ exhibits the best performance, with 50% IPA conversion (T50) at about 80 °C. T50 appears at about 210 °C and 230 °C for SnO_2 and Al_2O_3, respectively. For the three solids, the maximal overall IPA conversion reached is around 90%.

In order to select a system for fast IPA abatement, we investigated further the gas phase at reactor outlet during the heating ramp using the 1000 ppm IPA containing gas flow at the inlet
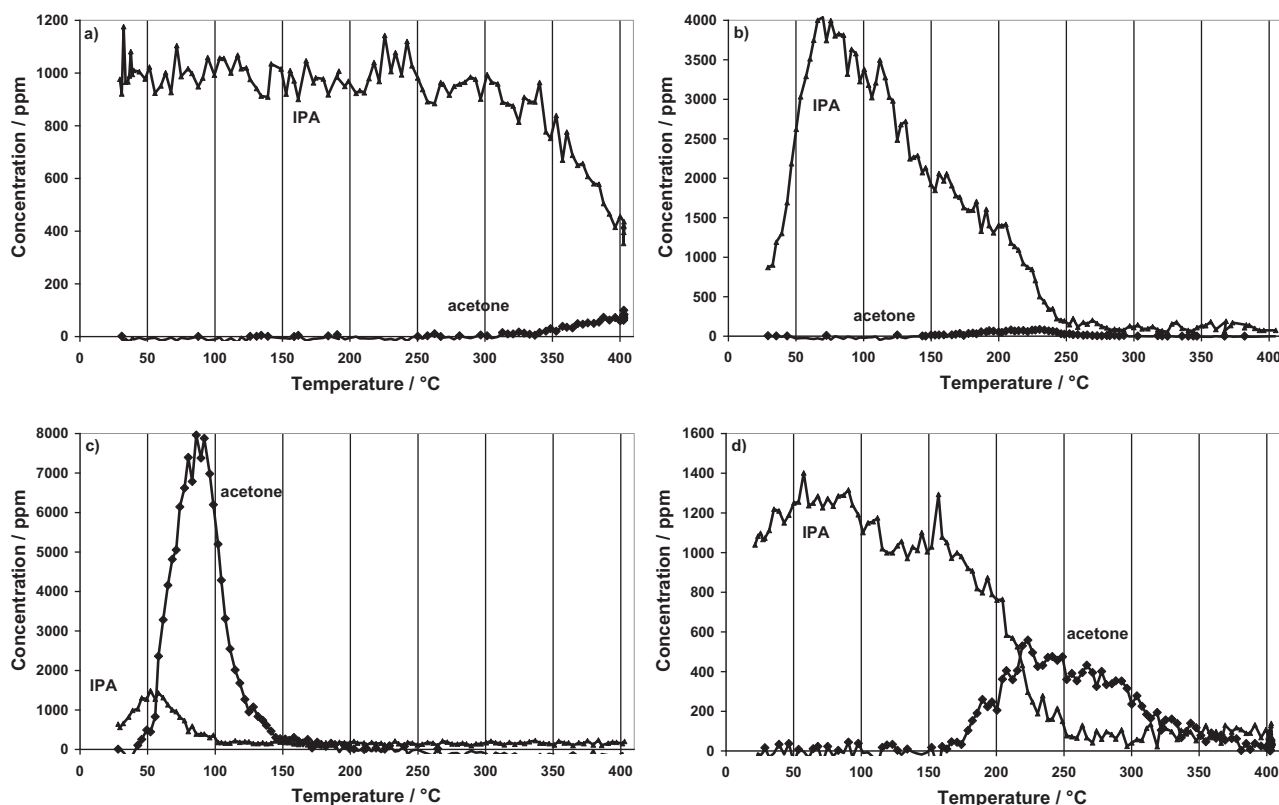
Fig. 6. IPA and acetone concentrations *vs* temperature on SS (a), Al_2O_3 on SS (b), $Pt-Al_2O_3$ on SS (c), and SnO_2 on SS (d). IPA initial concentration: 1000 ppm, heating rate: 20 °C min^{-1} and total flow rate: 100 NmL min-1.

of the reactor. The results reported in Fig. 6 show IPA and acetone concentrations vs temperature on SS (a), Al_2O_3 on SS (b), $Pt-Al_2O_3$ on SS (c), and SnO_2 on SS (d). On SS alone, neither IPA nor acetone desorption peak appears, IPA is only partially converted to acetone at high temperatures. This is in full agreement with the observation of Ilyas et al. [38], who reported the conversion of IPA toward acetone over Cr_2O_3 powder at 200 °C in a flowing microcatalytic reactor. The authors reported an appreciable steady-state catalytic activity only when oxygen was present in the reactant gas flow. On Al_2O_3, a massive desorption of IPA is detected in the 40–250 °C range, with concentration in the flow as high as 4000 ppm. This peak is accompanied by a small acetone production in the range 150–250 °C, followed by CO_2 production at higher temperatures. On $Pt-Al_2O_3$, we also observe an IPA desorption peak in the range 30–100 °C with a maximum concentration value in the flow about 1500 ppm. Nevertheless, the main feature is acetone formation in the 50–150 °C range, the concentration of which can reach 8000 ppm. Above this temperature, IPA full oxidation into CO_2 and H_2O can process, in full agreement with the observation of Bianchi and coworkers on IPA photocatalytic abatement on TiO_2 [39]. Using experimental microkinetics tools, the authors described the strong competitive chemisorption between IPA_{ads} and a strongly adsorbed acetone species which controls the high selectivity in acetone of the photocatalytic oxidation process for high IPA coverage. In the case of the present study, one consequence is that increasing the heating rate leads to a shift towards higher temperatures of the IPA and acetone production peaks (IPA desorption reaches its maximum rate at about 200 °C when the sample is heated at 200 °C min^{-1}) and therefore the beginning of CO_2 production is shifted accordingly. It is interesting to compare the amounts of IPA and acetone evolved from Al_2O_3 and $Pt-Al_2O_3$. They are 79 µmol IPA and 2 µmol acetone for Al_2O_3 and 7 µmol IPA and 80 µmol acetone for $Pt-Al_2O_3$. The amounts

(IPA + acetone) for both solids are very close (81–87 µmol) and this observation strongly advocate a temperature-programmed surface reaction (TPSR) forming acetone on $Pt-Al_2O_3$ from an alumina surface fully saturated by IPA at room temperature. At last, SnO_2 does not exhibit any detectable IPA desorption (concentration remains about 1000 ppm) and a very moderate acetone production (about 400 ppm at 220 °C). Above this temperature, IPA is fully converted into CO_2. Once the pseudo steady-state is reached, propene and acetone concentrations were under our detection limit for Al_2O_3, $Pt-Al_2O_3$ and SnO_2 catalysts. Then we can assume that selectivity at this point is near 100% to H_2O and CO_2. The absence of CO was checked for using He instead of N_2 in an independent test. For SS alone, acetone was the main product detected.

### 3.3. Fast-response catalytic system

Due to its ability to fully oxidize IPA into CO_2 and H_2O with very few by-products and low IPA storage and desorption, SnO_2/SS is a good and cheap candidate to test the feasibility of fast abatement of high quantities of IPA in air. Obviously, SnO_2 shows lower performance than $Pt-Al_2O_3$ in terms of T50, but it does not lead to massive IPA and acetone (up to 8000 ppm in stream) desorption. The reactor equipped with SnO_2 catalyst supported on SS was fed with a flow consisting in 1%IPA in air with a total flow rate: 125 NmL min^{-1}. The goal of this experiment was to mimic an accidental air contamination, demanding a fast remediation. First of all, we have to check that SnO_2/SS performance is sufficient to achieve IPA abatement at such a concentration. Fig. 7 shows the light-off curve (% conversion vs temperature) for IPA combustion on pickled SS tube (a) and SnO_2-coated SS tube (b) with heating rate 20 °C min^{-1}. Curve (a) can be considered as a blank experiment. The use of SnO_2 catalyst allows a total IPA conversion to CO_2 and H_2O with a T50 at about 310 °C. Subsequent heating/cooling cycles show a good
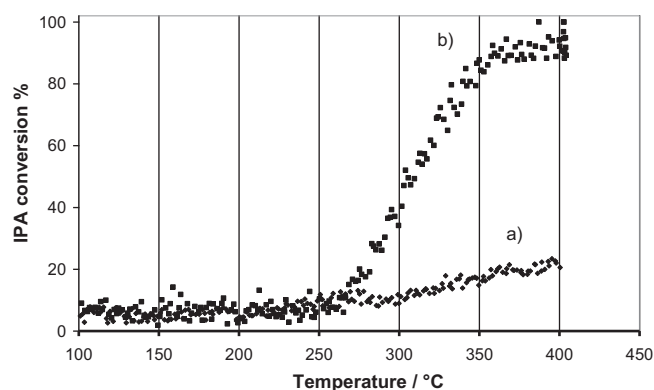
Fig. 7. Light-off curves for 1% IPA combustion in air on pickled SS (a) and on SnO$_2$ thin film deposited on SS (b). Heating rate: 20 °C min^{-1} and total flow rate: 125 NmL min^{-1}.
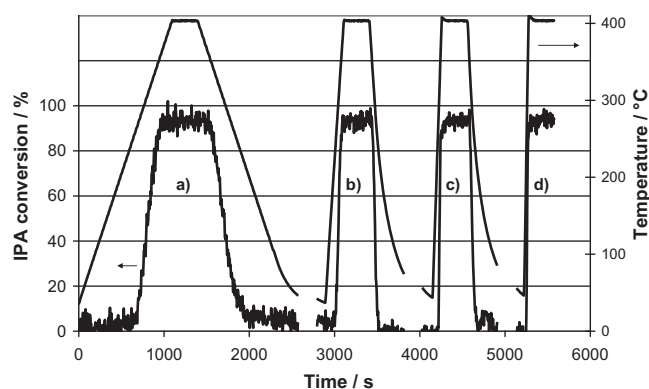
Fig. 8. Temperature of SnO$_2$-coated SS tube in air + 1% IPA flow and IPA conversion for heating rates: 20 (a), 100 (b), 200 (c), and 400 (d) °C min^{-1}. Total flow rate was 125 NmL min^{-1}.

repeatability of the catalytic performances. In order to check that IPA conversion is satisfactory at high heating rates IPA conversion was followed at 20 (a), 100 (b), 200 (c), and 400 (d) °C min^{-1} (see Fig. 8). Even at 400 °C min^{-1}, the performance for IPA abatement is satisfactory.

Fig. 9 shows IPA concentration at the inlet and the outlet of the reactor. The catalyst temperature is also shown. For this example, the heating rate was fixed at 800 °C min^{-1} and heating was started when the VOC signal was detected above a selected threshold at the reactor inlet. It is very interesting to note that total abatement
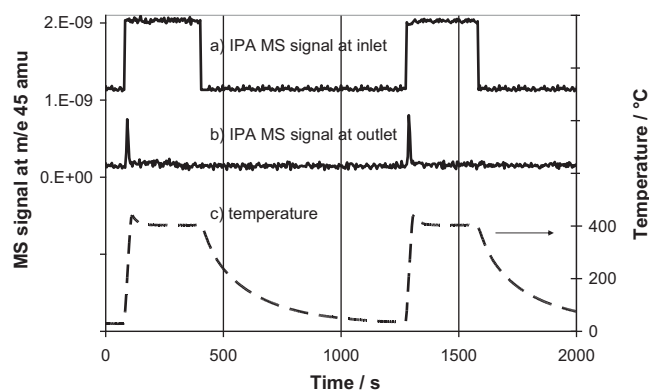
Fig. 9. IPA concentration at the inlet (a) and the outlet (b) of the reactor and catalyst temperature (c) vs time. Heating rate was fixed at 800 °C min^{-1} up to 400 °C. Signal (a) is offset to improve readability.

is reached in less than 30 s, starting with a catalyst at room temperature, and only CO$_2$ and H$_2$O are produced. When the inlet signal is decreased under the given threshold, induction heating is stopped and near-room temperature is recovered quickly.

4. Conclusions

This paper is the first publication of results obtained with an original setup consisting in a catalyst thin film deposited on a metallic support heated by an electromagnetic induction device. The feasibility and performances where demonstrated using a very commonly used metallic support such as stainless steel. Heating rates as high as 800 °C min^{-1} can be achieved with an accurate regulation in the range from room temperature to 400 °C. Obviously, much higher temperatures could be reached with this system, if necessary. Total abatement to CO$_2$ and H$_2$O of high amounts of IPA (about 1 vol%) in air was achieved in less than 30 s. Thermal inertia after induction shutting down is very low and room temperature can be recovered quickly. This shows the great practical interest of this system to achieve fast abatement of accidental contaminations especially in working places. The laboratory reactor described in this study was calculated to represent at the scale 1/1000 (in terms of catalyst mass and *ghsv*) what could happen if a 120 m^3 room was pumped at 300 m^3 h^{-1}. The corresponding real catalyst would be a monolith about 50 cm in length and 20 cm in dia. that could be efficiently heated by some inductive systems commonly used for metal surface treatment, for example.

The technique presented here makes also very feasible systems combining an adsorbent, that can be regenerated by flash desorption and a catalyst converting the desorbed species into H$_2$O and CO$_2$. Treating IPA by such a regenerative catalytic oxidizer using a conventional furnace was recently proposed by Lou and Huang [40].

From a more fundamental point of view, such a new system offers very interesting possibilities to study catalysts as thin films on structuring metals, to understand and model systems working under high *ghsv* and to accurately monitor the catalyst temperature, more particularly when studying very exothermic reactions.

References

[1] K. Everaert, J. Baeyens, Journal of Hazardous Materials B109 (2004) 113–139.
[2] S. Salvador, J.M. Commandré, Y. Kara, Applied Thermal Engineering 26 (2006) 2355–2366.
[3] K. Demeestere, J. Dewulf, H. Van Langenhove, Critical Reviews in Environment Science and Technology 37 (2007) 489–538.
[4] Z. He, J. Li, J. Chen, Z. Chen, G. Li, G. Sun, T. An, Chemical Engineering Journal 200–202 (2012) 645–653.
[5] J. Mo, Y. Zhang, Q. Xu, J. Joaquin Lamson, R. Zhao, Atmospheric Environment 43 (2009) 2229–2246.
[6] M.A. Sidheswaran, H. Destaillats, D.P. Sullivan, S. Cohn, W.J. Fisk, Building and Environment 47 (2012) 357–367.
[7] H.L. Chen, H.M. Lee, S.H. Chen, M.B. Chang, S.J. Yu, S.N. Li, Environmental Science & Technology 43 (2009) 2216–2227.
[8] S. Futamura, A. Zhang, H. Einaga, H. Kabashima, Catalysis Today 72 (2002) 259–265.
[9] R.R. Sadhankar, C.R. Aelick, D.L. Burns, K. Marcinkowska, Canadian Journal of Chemical Engineering 78 (2000) 1087–1095.
[10] R. Cherbański, E. Molga, Chemical Engineering and Processing 48 (2009) 48–58.
[11] E. Peillex, F. Gaillard, J.-P. Joly, M. Romand, Vacuum 59 (2000) 854–867.

[12] H. Ukai, S. Inui, S. Takada, J. Dendo, J. Ogawa, K. Isobe, T. Ashida, M. Tamura, K. Tabuki, M. Ikeda, International Archives of Occupational and Environmental Health 70 (1997) 385–392.

[13] J.W. Rosthauser, K. Nachtkamp, in: K.C. Frisch, D. Klempner (Eds.), Advances in Urethane: Science & Technology, vol. 10, Technomic Pub, Lancaster, PA, 1987, pp. 121–162.

[14] S. Seth, Y.C. Agrawal, P.K. Ghosh, D.S. Jayas, B.P.N. Singh, Biosystems Engineering 97 (2007) 209–217.

[15] A.J. Papa, Propanols, Ullmann's Encyclopedia of Industrial Chemistry, Wiley-VCH, Weinheim, 2005, http://dx.doi.org/10.1002/14356007.a22.173.

[16] A. Gervasini, A. Auroux, Journal of Catalysis 131 (1991) 190–198.

[17] J.E. Rekoske, M.A. Barteau, Journal of Catalysis 165 (1997) 57–72.

[18] J.A. Wang, X. Bokhimi, O. Novaro, T. Lopez, F. Tzompantzi, R. Gomez, J. Navarrete, M.E. Llanos, E. Lopez-Salinas, Journal of Molecular Catalysis A: Chemical 137 (1999) 239–252.

[19] V. Meille, Applied Catalysis A-General 315 (2006) 1–17.

[20] R. Wunsch, M. Fichtner, O. Gorke, K. Haas-Santo, K. Schubert, Chemical Engineering and Technology 25 (2002) 700–703.

[21] S.T. Aruna, K.S. Rajam, Materials Chemistry and Physics 111 (2008) 131–136.

[22] K. Belaroui, G. Rapillard, P. Bowen, H. Hofmann, V. Shklover, Ttp, Euro Ceramics VII (Pt 1–3), 2002, pp. 519–522.

[23] F. Gaillard, M. Romand, Surface and Interface Analysis 12 (1988) 491–496.

[24] F. Gaillard, J.P. Joly, A. Perrard, Adsorption Science & Technology 25 (2007) 245–256.

[25] .S. Parks, B. Barton, Journal of the American Chemical Society 50 (1928) 24–26.

[26] A. Beretta, G. Groppi, L. Majocchi, P. Forzatti, Applied Catalysis A-General 187 (1999) 49–60.

[27] G. Vincent, P.M. Marquaire, O. Zahraa, Journal of Hazardous Materials 161 (2009) 1173–1181.

[28] J.G. Mc Carty, Catalysis Today 26 (1995) 283–293.

[29] N. Doucet, F. Bocquillon, O. Zahraa, M. Bouchy, Chemosphere 65 (2006) 1188–1196.

[30] POLYPLUS, 39800 Poligny, France, www.polyplus.fr

[31] J.C. Luy, J.M. Parera, Applied Catalysis 26 (1986) 295.

[32] J. Cunningham, B.K. Hodnett, M. Iiyas, J. Tobin, E.L. Leahy, J.L. Fierro, Faraday Discussions 72 (1981) 283–302.

[33] M. Ai, J. Catal, Journal of Catalysis 50 (1977) 291.

[34] T. López, M. Asomoza, R. Gómez, Journal of Non-Crystalline Solids 147 (1992) 769.

[35] F. Gaillard, M. Romand, H. Hocquaux, J.S. Solomon, Surface and Interface Analysis 10 (1987) 163–167.

[36] H. Ma, Y. Berthier, P. Marcus, Corrosion Science 44 (2002) 171–178.

[37] F. Gaillard, J.P. Joly, E. Peillex, M. Romand, Journal of Adhesion 72 (3–4) (2000) 317–334.

[38] M. Ilyas, S. Shah, R. Nigat, H. Khan, Journal of the Chemical Society, Faraday Transactions 90 (1994) 2413–2415.

[39] F. Arsac, D. Bianchi, J.M. Chovelon, C. Ferronato, J.M. Herrmann, Journal of Physical Chemistry A 110 (2006) 4202–4212.

[40] J.C. Lou, S.W. Huang, Separation and Purification Technology 62 (2008) 71–78.